





Article

Supercritical CO₂-Assisted Electroless Plating of Ultrahigh-Molecular-Weight Polyethylene Filaments for Weavable Device Application

Hikaru Kondo¹, Tomoyuki Kurioka¹, Wan-Ting Chiu², Chun-Yi Chen¹, Jhen-Yang Wu^{1,*},
Tso-Fu Mark Chang^{1,*}, Machiko Yamaguchi³, Hiromichi Kurosu⁴ and Masato Sone¹

- ¹ Institute of Innovative Research, Tokyo Institute of Technology, Yokohama 226-8503, Japan; kondo.h.ai@m.titech.ac.jp (H.K.); kurioka.t.aa@m.titech.ac.jp (T.K.); chen.c.ac@m.titech.ac.jp (C.-Y.C.); sone.m.aa@m.titech.ac.jp (M.S.)
- ² Department of Materials Science and Engineering, Tokyo Institute of Technology, Tokyo 152-8550, Japan; chiu.w.aa@m.titech.ac.jp
- ³ Department of Clothing Environmental Science, Nara Women's University, Nara 630-8506, Japan; y.machiko76@gmail.com
- ⁴ Cooperative Major in Human Centered Engineering, Nara Women's University, Nara 630-8506, Japan; kurosu@cc.nara-wu.ac.jp
- * Correspondence: wu.j.ar@m.titech.ac.jp (J.-Y.W.); chang.m.aa@m.titech.ac.jp (T.-F.M.C.)

Abstract: This study reports on the use of supercritical CO₂ (scCO₂) for the metallization of ultrahigh-molecular-weight polyethylene (UHMW-PE) filaments, which are used as functional components in weavable devices. UHMW-PE is well known for its chemical and impact resistance, making it suitable for use in bulletproof clothing and shields. However, its chemical resistance poses a challenge for metallization. By utilizing scCO₂ as the solvent in the catalyzation process, a uniform and defect-free layer of Ni-P is successfully deposited on the UHMW-PE filaments. The deposition rate of Ni-P is enhanced at higher temperatures during the scCO₂ catalyzation. Importantly, the durability of the Ni-P-metallized UHMW-PE filaments is improved when the scCO₂ catalyzation is carried out at 120 °C, as evidenced by minimal changes in electrical resistivity after a rolling test.

Keywords: UHMW-PE; supercritical carbon dioxide; catalyzation temperature; Ni-P; metallization; electroless plating



Citation: Kondo, H.; Kurioka, T.; Chiu, W.-T.; Chen, C.-Y.; Wu, J.-Y.; Chang, T.-F.M.; Yamaguchi, M.; Kurosu, H.; Sone, M. Supercritical CO₂-Assisted Electroless Plating of Ultrahigh-Molecular-Weight Polyethylene Filaments for Weavable Device Application. *Electrochem* **2024**, *5*, 213–222. <https://doi.org/10.3390/electrochem5020013>

Academic Editor: Nikolay Dimitrov

Received: 2 May 2024

Revised: 19 May 2024

Accepted: 21 May 2024

Published: 3 June 2024



Copyright: © 2024 by the authors. Licensee MDPI, Basel, Switzerland. This article is an open access article distributed under the terms and conditions of the Creative Commons Attribution (CC BY) license (<https://creativecommons.org/licenses/by/4.0/>).

1. Introduction

In the recent years, there has been a rapid commercialization and practical use of wearable devices [1–3]. Wearable devices are worn on the body, such as on the arm, head, or clothing, and facilitate the measurement and transmission of vital signs. One promising area in wearable device technology is the interactive wearable device system [4], where textiles are endowed with chemical and physical sensing functions and the ability to elicit physical responses. To further enhance and expand the functionality of such wearable device systems, two or more types of filaments with different functions can be woven together to create a multifunctional wearable device, also known as a weavable device [5,6]. Functional filaments with good electrical conductivity are essential for weavable devices, which can be achieved through the metallization of polymer filaments. The integration of polymers and metals can be accomplished through various methods such as electroless plating [7–9], vacuum thermal evaporation [10,11], magnetron sputtering deposition [12], and chemical fluid deposition [13,14]. Electroless plating is preferred over evaporation techniques due to its low cost, relatively high deposition rate, and accessibility, as it does not require a vacuum environment like evaporation techniques.

Ensuring both sufficient electrical conductivity and stability in these metallized polymers for practical device application remains challenging because of the difference in

mechanical properties between the metal and polymer, and the difference often leads to insufficient adhesion between the two materials and defective results. Surface modification, such as plasma [10] and laser [15] treatments, of the polymer substrate is a solution to promote the adhesion before the metallization process. Recently, a metallization process by performing the catalyzation step of electroless plating in supercritical carbon dioxide (scCO₂) was reported to realize metallized polymer textiles possessing applicable electrical conductivity and adhesion properties between the metal and polymer toward functional components in flexible electronic devices. ScCO₂ is non-polar, and it has low viscosity, high self-diffusivity, and zero surface tension [16]. By these properties, scCO₂ has high affinity toward non-polar substances, such as polymers.

Generally, the process of electroless plating consists of three steps: a pretreatment step to clean and roughen the surface of the polymer substrate, a catalyzation step to decorate catalyst seeds on the polymer surface, and a metal deposition step to deposit metals on the polymer substrate. By utilizing scCO₂ as the solvent in the catalyzation step, the catalyst seeds can be inserted into the polymer structure [8,12]. Subsequently, the reduction and deposition of metals would be initiated from the catalyst seed inside the polymer structure. This results in metal structures extending into the polymer structure, leading to improved interactions between the polymer substrate and the metal coating. As a result of this improved interaction, the stability of the metallized polymer substrate is significantly enhanced while ensuring a decent electrical conductivity by the metal coating on the polymer substrate. The use of the scCO₂ catalyzation has been demonstrated in the metallization of nylon 6,6 textile, silk textile, and PET textile. The metal coatings deposited on these polymers are compact and smooth with high adhesion strength. Following the scCO₂-assisted electroless plating, the metallized polymer can be functionalized with a more electrically conductive metal, such as gold, or photocatalytic materials to realize flexible photocatalytic materials.

Ultrahigh-molecular-weight polyethylene (UHMW-PE) is a polymer that has gathered significant research interest for weavable devices due to its excellent chemical and mechanical properties, including low mass density, chemical resistance, abrasion resistance, high thermal conductivity, and impact resistance [17–19]. UHMW-PE filaments are commonly used in bulletproof vests, bedclothes, and protective gloves. The functionalization of UHMW-PE filaments with conductivity has potential applications in various fields, including medical sensors, smart textiles, and protective clothing [20]. However, the surface inactivity of UHMW-PE makes it challenging to metallize. Previous reports on the metallization of UHMW-PE have required a surface modification step, such as the use of dopamine [21] and electron beam continuous radiation-induced graft polymerization [22], before the catalyzation step to enable the deposition of metals on the UHMW-PE. Moreover, UHMW-PE filaments are known for their exceptional mechanical properties, making them highly suitable for demanding applications. According to Candadai et al. [17], UHMW-PE fibers exhibit remarkable tensile strength, abrasion resistance, and impact resistance, which are essential for weavable device application. Gao et al. further demonstrated that UHMW-PE fibers maintain high tensile strength and durability, reinforcing their suitability for integration into weavable technology [23]. These studies confirm that UHMW-PE filaments possess the mechanical robustness required for use in weavable devices, ensuring both durability and performance. The successful metallization of UHMW-PE filaments could lead to significant advancements in wearable technology, providing durable, conductive materials for a range of applications from healthcare monitoring devices to advanced military gear.

In this study, the Ni-P metallization of UHMW-PE filaments is achieved using scCO₂ catalyzation. Ni-P is chosen as the base material to allow for further functionalization of the UHMW-PE filaments. For instance, Ni-P can be used as the sacrificial material for deposition of a more electrically conductive and biocompatible gold layer]. Palladium(II) hexafluoroacetate is utilized as the palladium source due to its high solubility in

scCO₂ [24–27]. The durability of the Ni-P/UHMW-PE is evaluated through a rolling test, and the electrical resistivity of the Ni-P/UHMW-PE is measured to quantify its durability.

2. Materials and Methods

2.1. scCO₂-Assisted Ni-P Metallization of UHMW-PE Filament

The UHMW-PE filaments (IZANAS[®]) were procured from TOYOBO MC Co., Ltd. (Osaka, Japan). A custom-designed jig (refer to Figure 1) was utilized to support the filaments during the scCO₂ catalyzation to prevent entanglement. The jig was manufactured by the Design and Manufacturing Division, Open Facility Center, Tokyo Institute of Technology. The jig ensured that the UHMW-PE filaments were securely held in place, preventing them from tangling or contacting each other during the catalyzation process, which facilitated a uniform distribution of the catalyst on the filament surfaces. Palladium(II) hexafluoroacetylacetonate (Pd(hfa)₂; ≤100%) and ε-caprolactam (99%) were obtained from Sigma-Aldrich (Burlington, MA, USA). CO₂ (99.99%) was sourced from Taiyo Nippon Sanso Gas & Welding Corporation (Tokyo, Japan). The Ni-P deposition solution was supplied by Okuno Chemical Industries Co. (Osaka, Japan) and comprised nickel chloride (9 wt%), sodium hypophosphite (12 wt%), complexing agent (12 wt%), and ion-exchange water (67 wt%). The high-pressure CO₂ apparatus for the scCO₂ catalyzation was acquired from Japan Spectra Company (Tokyo, Japan), with a reaction cell volume of 50 mL.

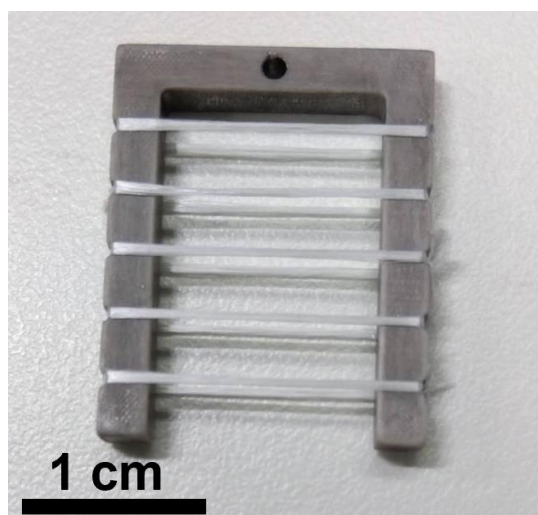


Figure 1. PEEK jig with the UHMW-PE filaments.

The UHMW-PE filaments were first sonicated in ethanol for 5 min and then dried in a box oven at 50 °C for 10 min prior to the scCO₂ catalyzation step. During the catalyzation step, the filaments, along with the jig, 50 mg of Pd(hfa)₂, 30 mg of ε-caprolactam, and a stir bar, were enclosed in the reaction cell. The stir bar was used to ensure a uniform distribution of the catalyst and ε-caprolactam, promoting an even distribution on the UHMW-PE filament surfaces for improved catalyzation efficiency and consistent metal deposition. The catalyzation was carried out for 2.0 h at a pressure of 15.0 MPa, using three different catalyzation temperatures, 80 °C, 100 °C, and 120 °C, taking into consideration the melting point of UHMW-PE, which is 136 °C. The Ni-P deposition was performed at atmospheric pressure and at a deposition temperature of 70 °C using the Ni-P electroless plating solution. The deposition time varied between 1 h, 2 h, and 3 h. No post-treatment was conducted after the Ni-P deposition.

Nonetheless, the scCO₂ catalyzation involves high-pressure conditions (15.0 MPa) and elevated temperatures (up to 120 °C), which could pose challenges related to equipment durability and safety. Additionally, the inherent chemical resistance and high melting point of UHMW-PE (136 °C) make the metallization process more complex. These factors must be carefully managed to ensure successful and consistent results. Furthermore,

the surface inactivity of UHMW-PE necessitates effective surface pretreatment to enable successful metallization.

2.2. Analyses of Surface and Physical Properties

The surface morphology of the catalyzed UHMW-PE and Ni-P/UHMW-PE was characterized using an optical microscope (OM, VHV-8000, KEYENCE, Osaka, Japan) and a scanning electron microscope (SEM, JSM-7500, JEOL, Tokyo, Japan). For observation of the cross-section, Ni-P/UHMW-PE filaments were mounted in epoxy and examined using the SEM. The constituent elements of the sample surface were identified using energy-dispersive X-ray spectroscopy (EDS; EMAX Evolution, HORIBA, Kyoto, Japan) equipped in the SEM. The crystal structures were identified using an X-ray diffractometer (XRD; Ultima IV, Rigaku, Tokyo, Japan).

The electrical resistivity was evaluated using a digital multimeter (CDM-27, CUSTOM, Tokyo, Japan) at room temperature. The two test probes of the digital multimeter were placed on the Ni-P/UHMW-PE filaments 10 mm apart to measure the electrical resistivity. Each specimen was measured five times. For the rolling test, the Ni-P metallized filaments were rolled around a cylinder with a 6 mm diameter, and the electrical resistivity was evaluated after unrolling the filaments.

3. Results and Discussion

The as-received UHMW-PE filaments were colorless and transparent, as depicted in Figure 2a. Following the scCO₂ catalyzation at 80 °C, the filaments exhibited an orange color, as shown in Figure 2b. The color of the as-received Pd(hfa)₂ lies between yellow and dark orange. Therefore, it is suggested that the observed orange color in the scCO₂ catalyzed filaments originated from the Pd(hfa)₂. As the catalyzation temperature increased to 100 °C and 120 °C, the color of the filaments gradually darkened, as shown in Figure 2c,d. It is reported that the thermal degradation of Pd(hfa)₂ to metallic Pd occurs in the temperature range of 90 °C to 150 °C at ambient pressure [27]. Small-sized metallic particles, such as small-sized Pd, appear black in color. Hence, the observed color change in the filaments catalyzed at higher temperatures is suggested to be due to the formation of metallic Pd from the Pd(hfa)₂. After the Ni-P deposition, all catalyzed UHMW-PE filaments exhibited a metallic luster, indicating successful Ni-P metallization of the scCO₂-catalyzed UHMW-PE filaments, as illustrated in Figure 2e–g.

SEM images of the UHMW-PE filaments catalyzed at different temperatures are depicted in Figure 3. In Figure 3a,b, agglomerations were observed on the surfaces of the filaments catalyzed at 80 °C. Considering the orange color observed in the scCO₂-catalyzed filaments, it is suggested that the agglomeration is Pd(hfa)₂. In Figure 3c,d, as the catalyzation temperature increased to 100 °C, the sizes of the agglomerations became smaller and more uniform. The filaments treated at 120 °C showed little or no agglomeration, as shown in Figure 3e,f.

Table 1 presents the results of the EDS analysis conducted on the filament surface following the scCO₂ catalyzation. The fluorine content was utilized as an indicator of the presence of Pd(hfa)₂ on the catalyzed filament surfaces, with EDS analysis performed at 10 different locations. The mean and standard deviation of the fluorine content were calculated. An observed decrease in the fluorine content was noted as the catalyzation temperature increased. At a catalyzation temperature of 120 °C, the fluorine content reached 0%, indicating a reduction in the amount of Pd(hfa)₂ on the filament surface. To further investigate the relationship between Pd(hfa)₂ reduction and catalyzation temperature, residue from the reaction cell after the scCO₂ catalyzation was analyzed using XRD. In Figure 4a,b, the (111) plane of the face-centered cubic (FCC) structure was observed in the residue treated at 100 °C, indicating the presence of Pd(111). The X-ray diffraction (XRD) results confirmed the formation of metallic Pd after catalyzation at 100 °C, supported by reference JCPDS Card No. 46-1043.

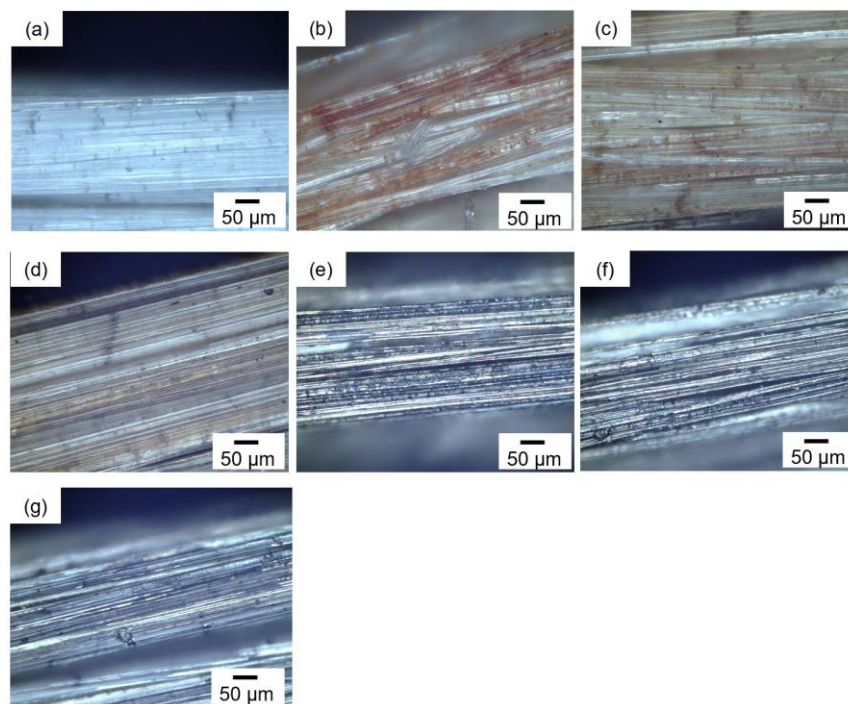


Figure 2. OM images of the (a) as-received UHMW-PE filaments, and UHMW-PE filaments catalyzed at (b) 80 °C, (c) 100 °C, and (d) 120 °C. The UHMW-PE filaments catalyzed (e) at 80 °C, (f) 100 °C, and (g) 120 °C after 1 h of Ni-P deposition.

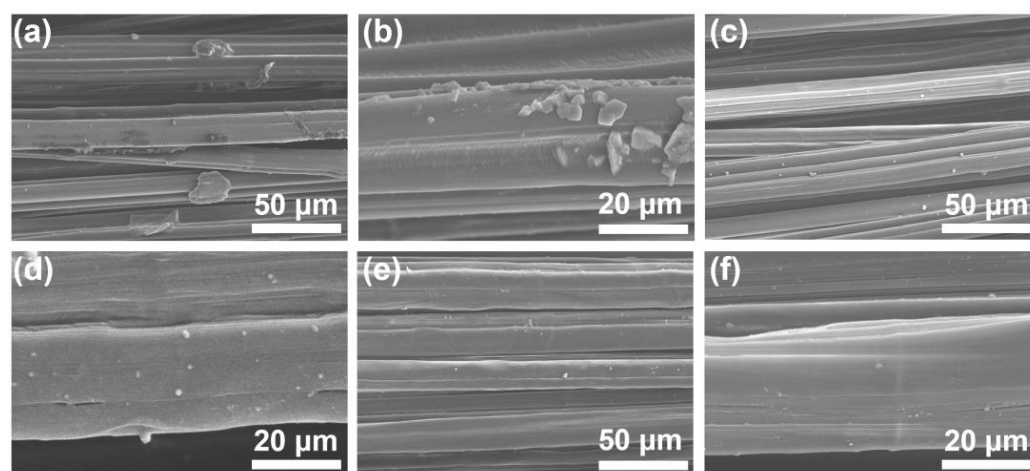


Figure 3. SEM images of the UHMW-PE filaments catalyzed at (a,b) 80 °C, (c,d) 100 °C, and (e,f) 120 °C.

Table 1. Fluorine content on surfaces of the UHMW-PE filaments after scCO₂ catalyzaion.

Catalyzaion Temperature	80 °C	100 °C	120 °C
Fluorine content	4.95 wt.%	1.29 wt.%	0 wt.%
Standard deviation	4.69 wt.%	2.30 wt.%	0 wt.%

The scCO₂ catalyzaion method is potentially scalable and cost-effective for industrial applications [28,29]. The use of non-toxic CO₂ and the elimination of hazardous chemicals enhance the safety and environmental friendliness of the process. The equipment and materials, including the high-pressure CO₂ apparatus and palladium catalyst, are commercially available and can be scaled up, making this method suitable for the large-scale production of metallized UHMW-PE filaments.

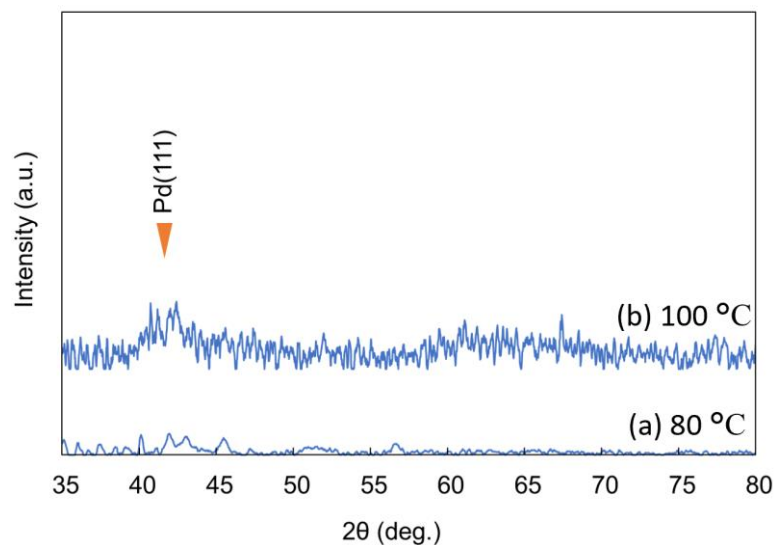


Figure 4. XRD patterns of the residue after scCO_2 catalyzed at (a) 80 °C and (b) 100 °C.

The SEM images in Figure 5 display the Ni-P-metallized UHMW-PE filaments catalyzed at varying temperatures. It is evident that all metallized filaments exhibit uniform surface conditions, regardless of the catalyzed temperature. No charging effect or defects were observed in any of the samples, indicating complete Ni-P metallization of the UHMW-PE filaments treated by scCO_2 catalyzed. Furthermore, the EDS analysis (Figure 6) confirmed that the entire surfaces were covered with a layer of Ni-P, with a Ni content and P content of 94.8 wt% and 5.2 wt%, respectively.

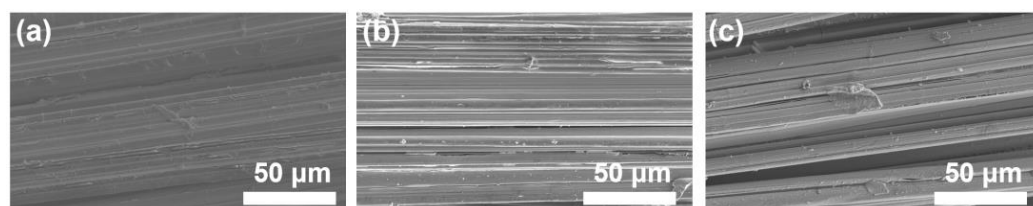


Figure 5. SEM images of the Ni-P-metallized UHMW-PE filaments with 1 h of deposition time and a catalyzed temperature of (a) 80 °C, (b) 100 °C, and (c) 120 °C.

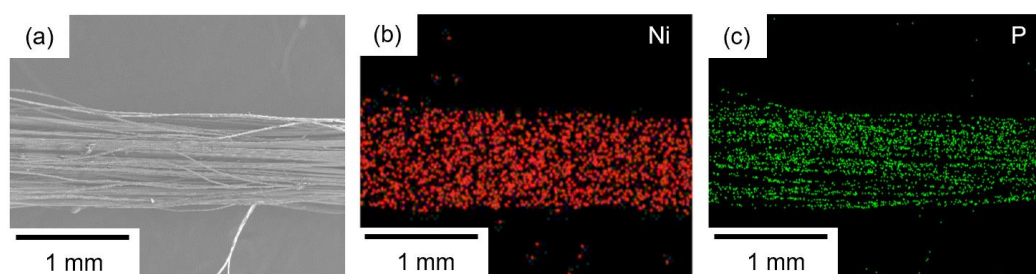


Figure 6. (a) SEM image and EDS mappings, and (b) Ni content and (c) P content on surfaces of the UHMW-PE filaments catalyzed at 80 °C with 1 h of the Ni-P deposition.

The enhancement in Ni-P deposition rate and durability at higher catalyzed temperatures can be attributed to the more efficient reduction of $\text{Pd}(\text{hfa})_2$ to metallic Pd, which serves as the catalyst for the Ni-P deposition. Higher temperatures facilitate the formation of well-dispersed Pd catalyst seeds, improving the uniformity and adhesion of the Ni-P coating. This results in a thicker, more consistent metal layer, thereby reducing electrical resistivity and increasing durability. The improved interactions between the metal coating and the polymer substrate at higher temperatures also contribute to the enhanced performance. The electrical resistivity values of Ni-P-metallized UHMW-PE are presented in

Figure 7. Two main effects can be observed from Figure 7a: the effects of catalyza-tion temperature and Ni-P deposition time. Firstly, a significant decrease in the electrical resistivity is observed with an increase in the catalyza-tion temperature, accompanied by a decrease in standard deviation of the electrical resistivity. The formation of Pd catalyst seeds on the surfaces of UHMW-PE filaments is crucial for initiating the deposition of Ni-P, which is achieved through the reduction of Pd(hfa)₂. This reduction can occur during the scCO₂ catalyza-tion step at high temperatures, or during the Ni-P deposition step using a reducing agent in the electroless plating solution. The results suggest that lower electrical resistivity is achieved when a high catalyza-tion temperature is used, indicating that the formation of Pd catalyst seeds in the scCO₂ catalyza-tion step is more effective.

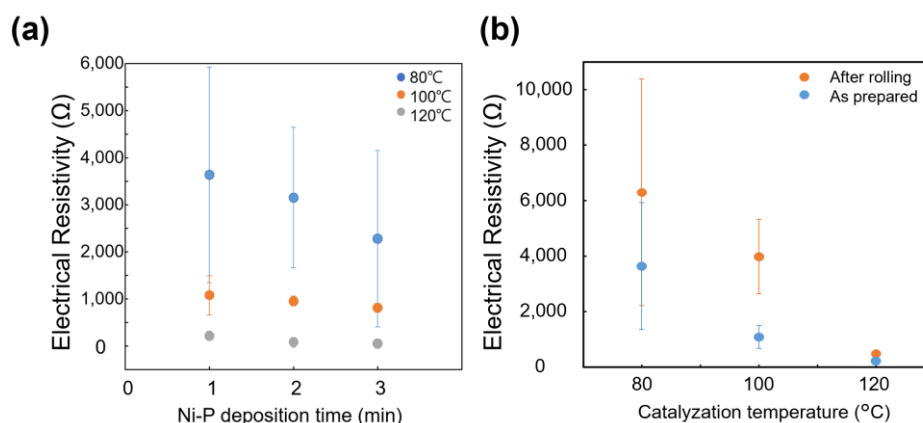


Figure 7. Electrical resistivity of (a) the Ni-P-metallized UHMW-PE and (b) the electrical resistivity of the UHMW-PE with 1 h of deposition time before and after the rolling test.

Regarding the effect of Ni-P deposition time, a decreasing trend in electrical resistivity is observed with prolonged deposition time. This trend is expected as a lower electrical resistivity is obtained with more Ni-P deposited on the surfaces. The lowest electrical resistivity of 48.0 Ω was achieved in the filaments catalyzed at 120 °C with 3 h of Ni-P deposition time.

The durability of Ni-P-metallized UHMW-PE filaments is demonstrated by the electrical resistivity after the rolling test. As shown in Figure 7b, both the electrical resistivity and the standard deviation increased after the rolling test, indicating deterioration of the Ni-P coatings due to the test. However, the deterioration was less severe when a higher catalyza-tion temperature was used. The electrical resistivity only slightly increased after the rolling test for the filaments catalyzed at 120 °C. These results highlight the advantages of the scCO₂ catalyza-tion with a high temperature in enhancing interactions between the metal coating and the polymer substrate.

Compared to other metallization methods, such as vacuum thermal evaporation and chemical fluid deposition, the scCO₂-assisted method provides significant advantages [30,31]. Traditional methods often require hazardous chemicals and complex equipment, whereas scCO₂ catalyza-tion uses non-toxic CO₂ and eliminates the need for a vacuum environment, making it safer and more environmentally friendly. Additionally, the efficient reduction of Pd(hfa)₂ and the subsequent formation of a uniform Ni-P coating at higher temperatures result in lower electrical resistivity and greater durability. These benefits underscore the practical applicability and superior performance of the scCO₂-assisted metallization process.

The impact of catalyza-tion temperature on the Ni-P-metallized filaments was further examined through cross-sectional SEM images, as illustrated in Figure 8a,b. The thickness of the Ni-P layer reached 0.34 μm for the filaments catalyzed at 80 °C after 1 h of the Ni-P deposition. Upon increasing the catalyza-tion temperature to 120 °C, the thickness escalated to 1.44 μm. This outcome confirms that the lower electrical resistivity observed in the metallized filaments catalyzed at higher temperatures is primarily due to a greater deposition of

Ni-P on the filament surface. Thus, a higher catalyzation temperature effectively enhances the rate of Ni-P deposition.

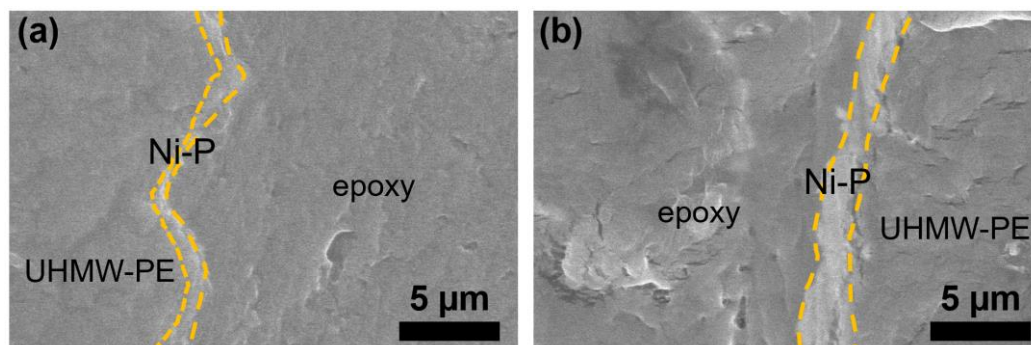


Figure 8. Cross-sectional SEM images of the Ni-P-metallized UHMW-PE filaments with the scCO₂ catalyzation at (a) 80 °C and (b) 120 °C and 1 h of Ni-P deposition time.

4. Conclusions

In this study, the Ni-P metallization of UHMW-PE filaments was achieved by conducting the catalyzation step in supercritical CO₂ and using palladium hexafluoroacetylacetonate as the source of the Pd catalyst seeds. Both optical microscopy observation and EDS analysis revealed changes in the surface conditions of the UHMW-PE filaments after the scCO₂ catalyzation step. The filament surfaces exhibited an orange color at a catalyzation temperature of 80 °C, which was attributed to the presence of Pd(hfa)₂. A dark color was observed on the surfaces at a catalyzation temperature of 120 °C, believed to be due to the presence of reduced Pd(hfa)₂. The change in the fluorine content on the surfaces and the XRD results further supported the reduction of Pd(hfa)₂ and the formation of metallic Pd at high catalyzation temperatures.

The Ni-P layer thickness increased from 0.34 μm to 1.44 μm with 1 h of the Ni-P deposition time when the catalyzation temperature increased from 80 °C to 120 °C. The high Ni-P deposition rate resulted in low electrical resistivity in filaments catalyzed at a high temperature. The high catalyzation temperature also improved the durability, as evidenced by the electrical resistivity after the rolling test. Also, a longer Ni-P deposition time caused a decrease in the electrical resistivity. The lowest electrical resistivity of 48.0 Ω was obtained in the UHMW-PE filaments catalyzed at 120 °C with 3 h of Ni-P deposition time. The improved Ni-P deposition rate and enhanced durability at high catalyzation temperature demonstrate the advantages of the scCO₂ catalyzation in the metallization of UHMW-PE filaments for the design of weavable devices.

These findings have significant implications for weavable device technology, particularly in enhancing the performance and reliability of weavable devices. Achieving uniform and durable metal coatings with low electrical resistivity is essential for the development of advanced wearable electronics and smart textiles. This work significantly contributes to the field by providing a scalable and environmentally friendly method for the metallization of UHMW-PE filaments through scCO₂ catalyzation.

Future research could explore different metal coatings to further enhance the electrical and mechanical properties of metallized UHMW-PE filaments and optimize the scCO₂ catalyzation process for other polymer substrates. Potential applications based on these findings include medical sensors, smart textiles, and protective clothing, where durable and conductive filaments are crucial. The demonstrated effectiveness of scCO₂ catalyzation in achieving durable and conductive coatings marks a significant advancement in the development of reliable and efficient weavable devices.

Author Contributions: Conceptualization, H.K. (Hiraku Kondo); Investigation, T.K., W.-T.C., C.-Y.C., J.-Y.W., T.-F.M.C., M.Y., H.K. (Hiromichi Kurosu), and M.S.; Writing—Original Draft Preparation, H.K. (Hiraku Kondo); Writing—Review and Editing, J.-Y.W. and T.-F.M.C. All authors have read and agreed to the published version of the manuscript.

Funding: This work was supported by the “Innovation inspired by Nature” Research Support Program, SEKISUI CHEMICAL Co., Ltd. (Tokyo, Japan); the Research Center for Biomedical Engineering, Tokyo Institute of Technology; and JSPS KAKENHI, Grant Numbers JP21H01668 and JP21H00807.

Institutional Review Board Statement: Not applicable.

Informed Consent Statement: Not applicable.

Data Availability Statement: The raw data supporting the conclusions of this article will be made available by the authors on request.

Acknowledgments: The authors would like to thank Murata in the Design and Manufacturing Division, Open Facility Center, Tokyo Institute of Technology, for preparing the jig.

Conflicts of Interest: The authors declare no conflicts of interest. The funders had no role in the design of the study; in the collection, analyses, or interpretation of data; in the writing of the manuscript; or in the decision to publish the results.

References

1. Patel, M.S.; Asch, D.A.; Volpp, K.G. Wearable Devices as Facilitators, Not Drivers, of Health Behavior Change. *JAMA* **2015**, *313*, 459–460. [[CrossRef](#)] [[PubMed](#)]
2. Seneviratne, S.; Hu, Y.; Nguyen, T.; Lan, G.; Khalifa, S.; Thilakarathna, K.; Hassan, M.; Seneviratne, A. A Survey of Wearable Devices and Challenges. *IEEE Commun. Surv. Tutor.* **2017**, *19*, 2573–2620. [[CrossRef](#)]
3. Fernández-Caramés, T.M.; Fraga-Lamas, P. Towards The Internet of Smart Clothing: A Review on IoT Wearables and Garments for Creating Intelligent Connected E-Textiles. *Electronics* **2018**, *7*, 405. [[CrossRef](#)]
4. Wang, Q.; Markopoulos, P.; Yu, B.; Chen, W.; Timmermans, A. Interactive Wearable Systems for Upper Body Rehabilitation: A Systematic Review. *J. NeuroEng. Rehabil.* **2017**, *14*, 20. [[CrossRef](#)]
5. Harrison, D.; Qiu, F.; Fyson, J.; Xu, Y.; Evans, P.; Southee, D. A Coaxial Single Fibre Supercapacitor for Energy Storage. *Phys. Chem. Chem. Phys.* **2013**, *15*, 12215–12219. [[CrossRef](#)] [[PubMed](#)]
6. Sun, G.; Liu, J.; Zheng, L.; Huang, W.; Zhang, H. Preparation of Weavable, All-Carbon Fibers for Non-Volatile Memory Devices. *Angew. Chem.* **2013**, *125*, 13593–13597. [[CrossRef](#)]
7. Mallory, G.O.; Hajdu, J.B. *Electroless Plating: Fundamentals and Applications*; William Andrew: Norwich, NY, USA, 1990; ISBN 978-0-936569-07-9.
8. Domenech, S.C.; Lima, E.; Drago, V.; De Lima, J.C.; Borges, N.G.; Avila, A.O.V.; Soldi, V. Electroless Plating of Nickel–Phosphorous on Surface-Modified Poly(Ethylene Terephthalate) Films. *Appl. Surf. Sci.* **2003**, *220*, 238–250. [[CrossRef](#)]
9. Adachi, H.; Taki, K.; Nagamine, S.; Yusa, A.; Ohshima, M. Supercritical Carbon Dioxide Assisted Electroless Plating on Thermoplastic Polymers. *J. Supercrit. Fluids* **2009**, *49*, 265–270. [[CrossRef](#)]
10. Petit, S.; Laurens, P.; Amouroux, J.; Arefi-Khonsari, F. Excimer Laser Treatment of PET before Plasma Metallization. *Appl. Surf. Sci.* **2000**, *168*, 300–303. [[CrossRef](#)]
11. Gupta, S.; Dixit, M.; Sharma, K.; Saxena, N.S. Mechanical Study of Metallized Polyethylene Terephthalate (PET) Films. *Surf. Coat. Technol.* **2009**, *204*, 661–666. [[CrossRef](#)]
12. Amberg, M.; Grieder, K.; Barbadoro, P.; Heuberger, M.; Hegemann, D. Electromechanical Behavior of Nanoscale Silver Coatings on PET Fibers. *Plasma Process. Polym.* **2008**, *5*, 874–880. [[CrossRef](#)]
13. Wei, Q.; You, E.; Hendricks, N.R.; Briseno, A.L.; Watkins, J.J. Flexible Low-Voltage Polymer Thin-Film Transistors Using Supercritical CO₂-Deposited ZrO₂ Dielectrics. *ACS Appl. Mater. Interfaces* **2012**, *4*, 2322–2324. [[CrossRef](#)]
14. Blackburn, J.M.; Long, D.P.; Cabañas, A.; Watkins, J.J. Deposition of Conformal Copper and Nickel Films from Supercritical Carbon Dioxide. *Science* **2001**, *294*, 141–145. [[CrossRef](#)]
15. Rozovskis, G.; Vinkevičius, J.; Jačiauskienė, J. Plasma Surface Modification of Polyimide for Improving Adhesion to Electroless Copper Coatings. *J. Adhes. Sci. Technol.* **1996**, *10*, 399–406. [[CrossRef](#)]
16. Clifford, T. *Fundamentals of Supercritical Fluids*; Oxford University Press: Oxford, UK, 1998; ISBN 978-1-383-02001-4.
17. Candadai, A.A.; Nadler, E.J.; Burke, J.S.; Weibel, J.A.; Marconnet, A.M. Thermal and Mechanical Characterization of High Performance Polymer Fabrics for Applications in Wearable Devices. *Sci. Rep.* **2021**, *11*, 8705. [[CrossRef](#)]
18. Shi, J.; Liu, S.; Zhang, L.; Yang, B.; Shu, L.; Yang, Y.; Ren, M.; Wang, Y.; Chen, J.; Chen, W.; et al. Smart Textile-Integrated Microelectronic Systems for Wearable Applications. *Adv. Mater.* **2020**, *32*, 1901958. [[CrossRef](#)]
19. Zhang, W.; Hu, Z.; Zhang, Y.; Lu, C.; Deng, Y. Gel-Spun Fibers from Magnesium Hydroxide Nanoparticles and UHMWPE Nanocomposite: The Physical and Flammability Properties. *Compos. Part B Eng.* **2013**, *51*, 276–281. [[CrossRef](#)]

20. Avcı, H.; Hassanin, A.; Hamouda, T.; Kiliç, A. High Performance Fibers: A Review on Current State of Art and Future Challenges. *Eskişehir. Osman. Üniversitesi Mühendis. Mimar. Fakültesi Derg.* **2019**, *27*, 130–155. [[CrossRef](#)]
21. Hu, W.; Zeng, Z.; Wang, Z.; Liu, C.; Wu, X.; Gu, Q. Facile Fabrication of Conductive Ultrahigh Molecular Weight Polyethylene Fibers via Mussel-Inspired Deposition. *J. Appl. Polym. Sci.* **2013**, *128*, 1030–1035. [[CrossRef](#)]
22. Gao, Q.; Hu, J.; Yang, Y.; Wang, M.; Zhang, M.; Tang, Z.; Zhang, M.; Liu, W.; Wu, G. Fabrication of New High-Performance UHMWPE-Based Conductive Fibers in a Universal Process. *Ind. Eng. Chem. Res.* **2019**, *58*, 935–943. [[CrossRef](#)]
23. Zhang, K.; Li, W.; Zheng, Y.; Yao, W.; Zhao, C. Compressive Properties and Constitutive Model of Semicrystalline Polyethylene. *Polymers* **2021**, *13*, 2895. [[CrossRef](#)]
24. Higashi, H.; Iwai, Y.; Miyazaki, K.; Ogino, Y.; Oki, M.; Arai, Y. Measurement and Correlation of Solubilities for Trifluoromethylbenzoic Acid Isomers in Supercritical Carbon Dioxide. *J. Supercrit. Fluids* **2005**, *33*, 15–20. [[CrossRef](#)]
25. Shimoyama, Y.; Sonoda, M.; Miyazaki, K.; Higashi, H.; Iwai, Y.; Arai, Y. Measurement of Solubilities for Rhodium Complexes and Phosphine Ligands in Supercritical Carbon Dioxide. *J. Supercrit. Fluids* **2008**, *44*, 266–272. [[CrossRef](#)]
26. Tenorio, M.J.; Cabañas, A.; Pando, C.; Renuncio, J.A.R. Solubility of Pd(Hfac)₂ and Ni(Hfac)₂·2H₂O in Supercritical Carbon Dioxide Pure and Modified with Ethanol. *J. Supercrit. Fluids* **2012**, *70*, 106–111. [[CrossRef](#)]
27. Zhao, X.; Hirogaki, K.; Tabata, I.; Okubayashi, S.; Hori, T. A New Method of Producing Conductive Aramid Fibers Using Supercritical Carbon Dioxide. *Surf. Coat. Technol.* **2006**, *201*, 628–636. [[CrossRef](#)]
28. Seifzadeh, D.; Mohsenabadi, H.K.; Rajabalizadeh, Z. Electroless Ni–P Plating on Magnesium Alloy by Innovative, Simple and Non-Toxic Oxalate Pretreatment and Its Corrosion Protection. *RSC Adv.* **2016**, *6*, 97241–97252. [[CrossRef](#)]
29. Hernandha, R.F.H.; Rath, P.C.; Umesh, B.; Patra, J.; Huang, C.-Y.; Wu, W.-W.; Dong, Q.-F.; Li, J.; Chang, J.-K. Supercritical CO₂-Assisted SiO_x/Carbon Multi-Layer Coating on Si Anode for Lithium-Ion Batteries. *Adv. Funct. Mater.* **2021**, *31*, 2104135. [[CrossRef](#)]
30. Bozbag, S.E.; Sanli, D.; Erkey, C. Synthesis of Nanostructured Materials Using Supercritical CO₂: Part II. Chemical Transformations. *J. Mater. Sci.* **2012**, *47*, 3469–3492. [[CrossRef](#)]
31. Romang, A.H.; Watkins, J.J. Supercritical Fluids for the Fabrication of Semiconductor Devices: Emerging or Missed Opportunities? *Chem. Rev.* **2010**, *110*, 459–478. [[CrossRef](#)]

Disclaimer/Publisher’s Note: The statements, opinions and data contained in all publications are solely those of the individual author(s) and contributor(s) and not of MDPI and/or the editor(s). MDPI and/or the editor(s) disclaim responsibility for any injury to people or property resulting from any ideas, methods, instructions or products referred to in the content.